Journal of the European Ceramic Society **12** (1993) 71–77

A Novel Method to Determine the *R*-Curve Behaviour of Ceramic Materials: Application to a Ceria-Partially Stabilized Zirconia

J. C. Descamps, A. Poulet

Materials Science Department, Polytechnic Faculty of Mons, Rue de l'Epargne, 56, 7000 Mons, Belgium

P. Descamps & F. Cambier

Belgian Ceramic Research Centre, Avenue Gouverneur Cornez, 4, 7000 Mons, Belgium

(Received 22 July 1992; revised version received 13 November 1992; accepted 11 December 1992)

Abstract

A new method, allowing the determination of R-curve behaviour of ceramic materials, is developed. This method, called 'crack line wedge loading' (CLWL), presents many advantages, especially the continuous observation of the crack growth, a mode 1 fracture specimen and plane stress, conditions favourable to show the rising R-curve effect. The R-curve behaviour of Ce-ZrO_2 is assessed by this new test procedure and the results are compared with those given by another classical method (Bluhm's slice model). The data obtained by the two methods are in close agreement. However, the new method allows a broader range of crack lengths to be covered and thus is a more accurate technique to determine the stress intensity factor corresponding to the crack initiation. It is shown that the CLWL technique gives actual values of the stress intensity factor because it is possible to take into account the main crack, together with the microcracks constituting the process zone.

Eine neue Methode zur Bestimmung des R-Kurvenverhaltens von keramischen Werkstoffen wird entwickelt. Diese Methode, 'crack line wedge loading' (CLWL) genannt, hat viele Vorteile. Sie erlaubt unter anderem eine kontinuierliche Beobachtung des Rißwachstums, die Verwendung von Mode 1 Bruchproben und des ebenen Spannungszustandes. Dies ermöglicht es, den Effekt einer ansteigenden R-Kurve zu zeigen. Das R-Kurvenverhalten von Ce-ZrO_2 wird mit Hilfe dieser neuen Testmethode abgeschätzt, und die Ergebnisse werden mit denen einer anderen, klassischen Methode (Bluhm's Scheibenmodell) verglichen. Die Ergebnisse beider Methoden sind in guter Übereinstimmung. Jedoch erlaubt die neue Methode die Untersuchung eines größeren Rißlängenspektrums und ist somit eine präzisere Technik zur Bestimmung des Spannungsintensitätsfaktors bezüglich der Rißeinleitung. Es wird gezeigt, daß die CLWL-Technik den tatsächlichen Wert des Spannungsintensitätsfaktors ergibt, weil es möglich ist, den Hauptriß zusammen mit den Mikrorissen, die die Prozeßzone bilden, zu berücksichtigen.

Une nouvelle technique, permettant de déterminer les courbes-R de matériaux céramiques présentant une consolidation, a été développée. Cette technique, appelée 'crack-line wedge loading' (CLWL), offre de nombreux avantages, tels que la visualisation continue de la fissuration, la sollicitation de l'éprouvette en mode 1, en état plan de contrainte (condition idéale de mise en évidence d'un effet de courbe-R). L'application de cette méthode pour l'étude d'une zircone cériée nous a permis de mettre en évidence toute son efficacité; à titre de comparaison, nous avons appliqué la méthode classique développée par Bluhm et nous avons discuté les résultats. Un des aspects les plus intéressant de la nouvelle technique est qu'elle permet de tenir compte à la fois de la macrofissure ainsi que de la zone microfissurée qui apparaît au front de propagation, ce qui rend la caractérisation du matériau plus rigoureuse à partir de la connaissance de son facteur d'intensité de contrainte.

1 Introduction

Ceramic materials are generally brittle. To improve their rupture behaviour, many research works are

Journal of the European Ceramic Society 0955-2219/93/$6.00

currently devoted to the development of new ceramics or new ceramic composites showing special microstructure or texture, which allow reinforcing mechanisms to occur.

However, to characterize the rupture of such materials, which often present a non-linear crack resistance behaviour (*R*-curve), most of the methods used today are based on three- or four-point bending tests; one exception is the technique recently proposed by Calomino & Brewer.[1]

Bending tests are far from true mode 1 cracking and do not lead to an easy control of stable crack propagation. Therefore, on the basis of experience carried out on metal testing, a novel method has been developed, allowing:

—A quantitative study of stable crack growth in ceramic materials;
—the reinforcement mechanisms to be shown;
—from a preponderant reproducible flaw, the crack to be shown to be propagating through the ceramic material.

The testing device and the data analysis method were applied to the study of crack behaviour of a ceria-partially stabilized zirconia (Ce-PSZ) ceramic. The properties of this material are given first in terms of physical and mechanical characteristics; secondly, the new technique and the data obtained from it are described, and finally are discussed.

2 Processing and Characteristics of the Ceria-Stabilized Zirconia Ceramic

2.1 Processing

The starting powder (Unitec PSZ-Ce 14, Unitec Ceramics Ltd, UK) has the following chemical composition (wt%): ZrO_2 85·5, CeO_2 14, and MgO, Al_2O_3, SiO_2, Fe_2O_3, Na_2O each less than 0·1. Its grain size distribution was assessed by laser diffraction (Malvern MasterSizer, UK), giving an average diameter (d_{50}) of 0·65 μm and a d_{95} of 1·5 μm. Specific surface area (BET) was 7·2 $m^2 g^{-1}$. Its mineralogical content, obtained from X-ray diffraction (Smith & Newkirk equation[2]) was 79 vol.% monoclinic and 21 vol.% tetragonal.

The raw materials were isostatically pressed in silicon moulds, under 170 MPa, giving $65 \times 55 \times 50\,mm^3$ parallelepipeds, which were sintered under air following the schedule:

—20–900°C: heating rate 1°C min^{-1};
—900–1500°C: heating rate 7·5°C min^{-1};
—dwell time: 2 h;
—1500–room temperature: cooling rate 7·5°C min^{-1}.

The densified material was cut into 4 mm thick plates using diamond wheels and machined thereafter to give the geometry described later in Fig. 5.

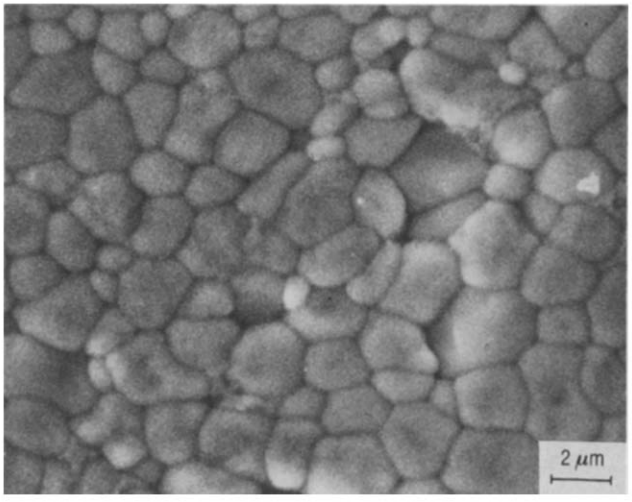

Fig. 1. SEM picture of a thermally etched polished surface of the Ce-partially stabilized zirconia.

2.2 Physical properties

After sintering, the bulk density, measured by Archimedes' method, was $6{\cdot}17 \times 10^3\,kg\,m^{-3}$ and open porosity was close to 0%.

A typical picture, representing the obtained microstructure, is given in Fig. 1. It shows the homogeneous distribution of polygonal grains. It corresponds to the scanning electron microscopy image of a polished surface, thermally etched at 1500°C for 15 min. The image analysis of a set of similar pictures gave an average grain area of 3 μm^2 and an average grain diameter of 2·7 μm, taking into account Abercrombie's correction.[3]

The tetragonal zirconia content was estimated to 42% (by the same method as for powders).[2]

The intrinsic elastic properties were also measured on plates: the longitudinal elastic (Young's) modulus was estimated using both an ultrasonic propagation rate method and a resonant frequency technique (Grindo-Sonic). The mean value was 188 ± 8 GPa. Using the same ultrasonic method, the transverse elastic (shear) modulus G was estimated to be 72 ± 4 GPa. From these values, Poisson's ratio was calculated to be 0·31.

2.3 Mechanical properties

The material was characterized from a mechanical point of view: microhardness, strength and toughness values were assessed and the results are summarized in Table 1. Microhardness measure-

Table 1. Mechanical properties of Ce-PSZ material

HV_{5N}	σF (MPa)	K_{Ii} (MPa$\sqrt{m}$)	K_{IC} (MPa$\sqrt{m}$)
890 ± 25	302 ± 20	$7{\cdot}1 \pm 0{\cdot}5$	$12 \pm 0{\cdot}5$

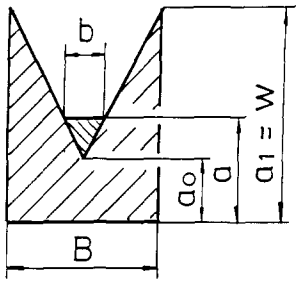

Fig. 2. Geometry of a three-point bend chevron notch specimen (Bluhm's slice model: $w = 4{\cdot}1$ mm; $B = 3$ mm; $a_0 = 1{\cdot}26$ mm; $a_1 = w$).

ment was performed using a 136° Vickers pyramidal indenter and an applied load of 5 N. Strength was measured by a three-point flexural test in accordance with the R 1601–1981 Japanese standard.

Fracture toughness was determined from three-point bend specimens having a chevron notch (CN) machined in their centre (Fig. 2). This CN technique was chosen because it does not require the ambiguous measurement of the initial crack length and allows the problem of K_{IC} dependence on the notch width encountered with straight-through notched specimens (typically in the SENB method) to be avoided. The load was recorded as a function of the beam deflection and K_{IC} calculation was made following the Bluhms' slice model, as described by Munz *et al.*[4]

Processing of load–displacement data gives rise to the K_R versus a/w curve of Fig. 3, corresponding to mode I crack growth in plane strain. The stress intensity factor relative to crack initiation (K_{Ii}) was found to be $7{\cdot}1 \pm 0{\cdot}5$ MPa $\sqrt{m}$, whereas the critical value corresponding to unstable crack growth (K_{IC}) was $12 \pm 0{\cdot}5$ MPa $\sqrt{m}$.

3 *R*-Curve Determination

3.1 The Crack-Line-Wedge-Loading method

Numerous standardized methods are available for the determination of *R*-curves of metallic materials (American National Standards).

Among these methods, the crack line wedge loading (CLWL) technique[5] was considered to be the most suitable choice for ceramic materials characterized by a stable crack growth. Taking into account noticeable adjustments in shape and size of both the specimen and the loading configuration, this method presents the following advantages:

—It is close to plane stress conditions, favourable for highlighting the rising *R*-curve effect;
—fracture occurs according to mode 1 crack growth;
—it allows a direct observation of the stable crack growth.

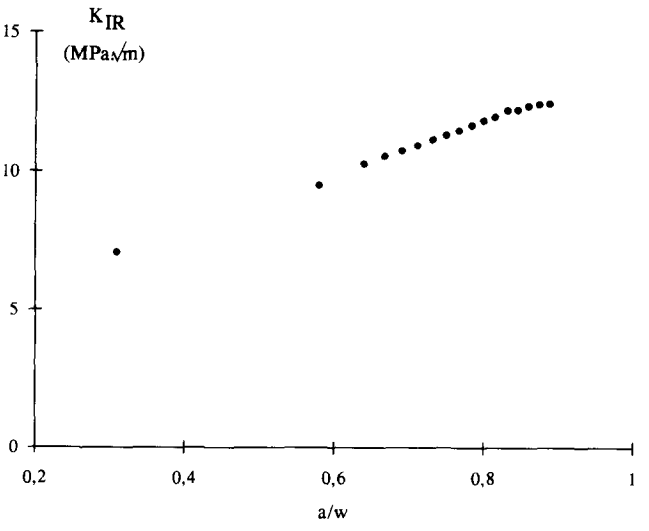

Fig. 3. Typical *R*-curve from three-point flexural test on a chevron notch specimen.

3.2 Description of the experimental procedure

The loading configuration used for experiments is shown in Fig. 4. The testing device consists mainly of:

—A low taper-angle wedge, with a polished surface finishing. The angle of the wedge may be chosen as depending on the tested material and was fixed in the present work at a value of 3°; this value is in agreement with standard advice.
—A split-pin system in order to maintain the load line independent of rotation of the specimen arms.

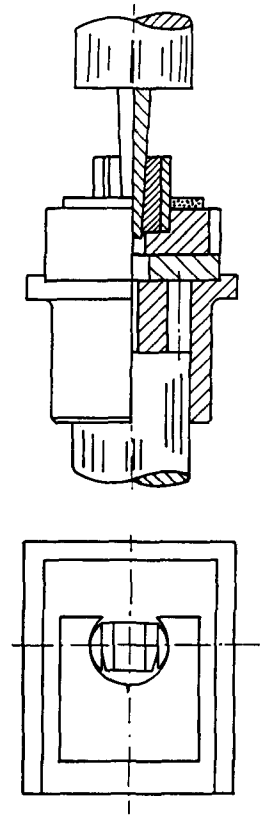

Fig. 4. CLWL testing device.

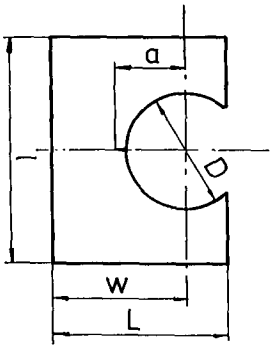

Fig. 5. CLWL specimen geometry ($w = 31{\cdot}5$ mm; $D = 26{\cdot}1$ mm; $L = 40{\cdot}0$ mm; $l = 52{\cdot}0$ mm; $B = 4{\cdot}0$ mm; $a_0 = 14{\cdot}75$ mm).

Specimens of various geometries have been tried. Best results were achieved with the test piece reported in Fig. 5 and having a dimensional ratio, as well as uncracked ligament length, in accordance with standard specification.

In order to induce a preponderant flaw, an initial notch was machined in the test piece by an ultrasonic drilling technique. This technique avoids any structural damages generated by saw cutting and allows reproducible slots to be obtained.

Special care was taken to adapt the sonotrode shape to the machining tool, consisting in a razor blade. A 35 vol.% SiC water slurry and a resonance frequency of 25 KHz were used. Using this technique, notch tip diameter of about 200 μm was obtained, such a width representing a reproducible flaw, allowing the investigation of the propagation behaviour.

Load versus time curves were recorded from experiments performed on a universal testing machine (Zwick 1474, Zwick GmbH, Germany)

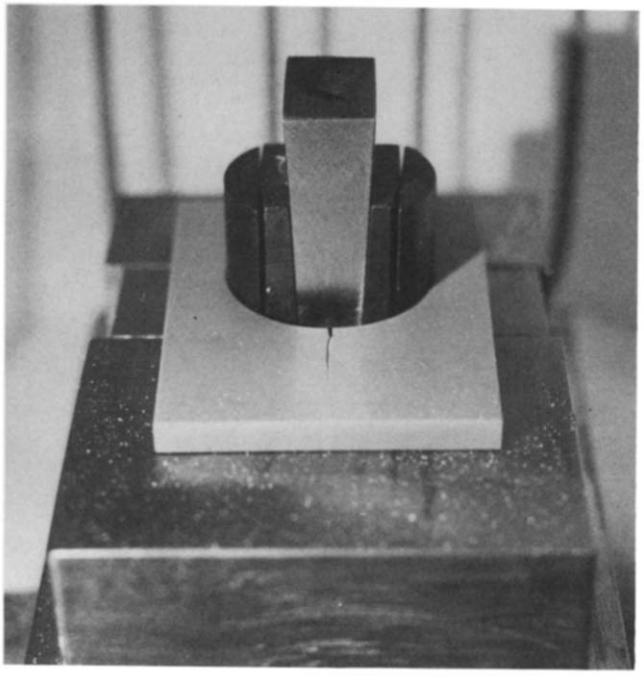

Fig. 6. Loading configuration.

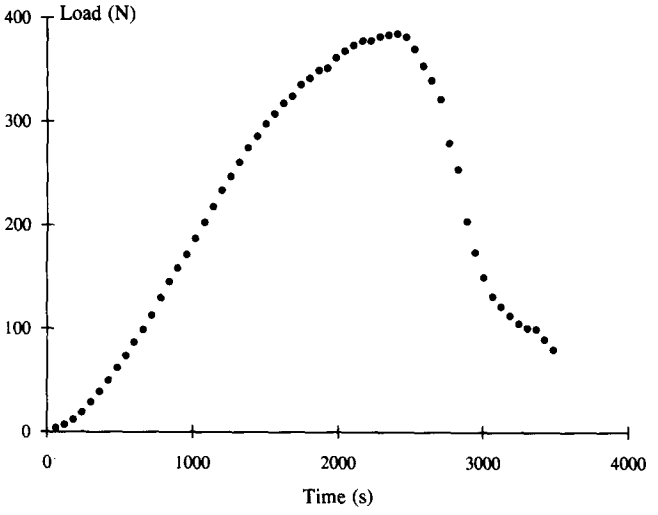

Fig. 7. Typical load versus time diagram.

equipped for compression test, using the loading configuration previously described (Fig. 6).

Tests were carried out at a constant crosshead speed of 50 μm min^{-1} and pictures of the crack were continuously taken during its growth.

4 Results and Discussion

A typical load versus time curve is presented, as recorded, in Fig. 7. It shows the non-linear crack resistance behaviour of the tested ceramic. From this curve, it can be noticed that:

—At the beginning, the load increases to reach a maximum value;
—after a sharp decrease, the load passes by an inflection point before decreasing more slowly.

During loading, taking into account the crack growth at the macroscopic scale, it can be pointed out that (Fig. 8):

—A main crack grows with time from the initial notch tip with a relatively straight trajectory parallel to the lateral sides of the specimen;
—a frontal zone of clearer colour develops at the main crack tip and extends all around its lateral faces. Scanning electron micrographs revealed that the clearer zone is largely composed of short cracks, here called microcracks to dist-

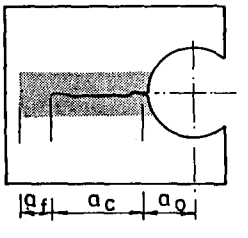

Fig. 8. Scheme of the crack growth. a_0 = Starting notch; a_c = macrocrack length; a_f = microcracked process zone size.

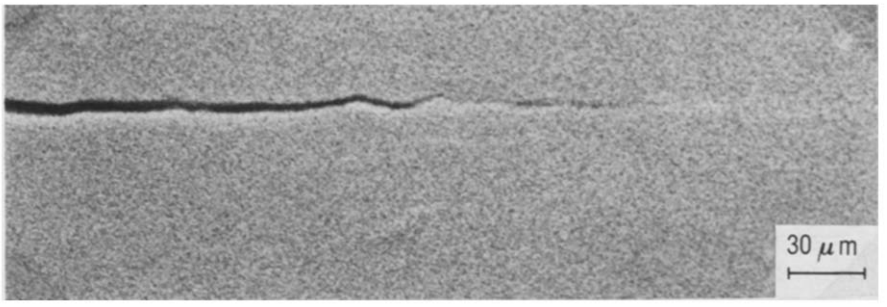

(a)

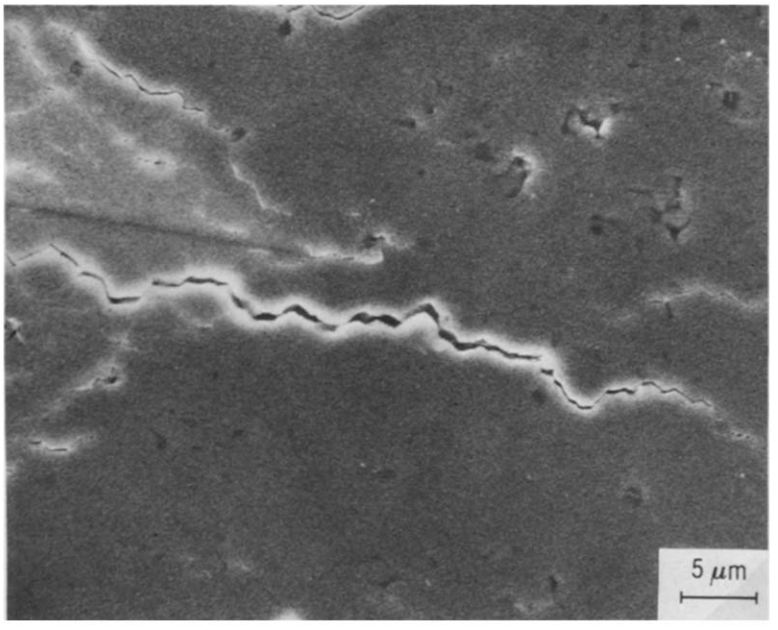

(b)

Fig. 9. (a) Picture of the macrocrack (optical microscopy); (b) magnification showing microcracks within the process zone (SEM micrograph).

inguish them from the main crack (Fig. 9). The presence of numerous microcracks influences the light reflection and is, as a consequence, responsible for colour contrasts observed at the specimen surface.

According to the foreseen observations, it is obvious that the crack length to be considered for calculation has to take the global form:

$$a = a_o + a_c + a_f$$

where a_o is the starting notch length, a_c the macrocrack length and a_f the size of the micro-cracked process zone at the main crack tip (these three parameters are experimentally measured on the same observation).

Figure 10 shows a typical example of crack propagation as a function of time in the Ce-zirconia ceramic studied; it also describes the corresponding evolution of the applied load (same as Fig. 7). Comparing those curves, it can be observed that they allow the phenomena to be split into several steps:

—From A0 to A1: the applied load is too low to induce a crack from the slot;

—from A1 to A2: the velocity of the crack propagation increases until the load reaches its maximum;

—from A2 to A3: the velocity increases faster than in the previous step and the load versus time curve passes by the inflection point A3;

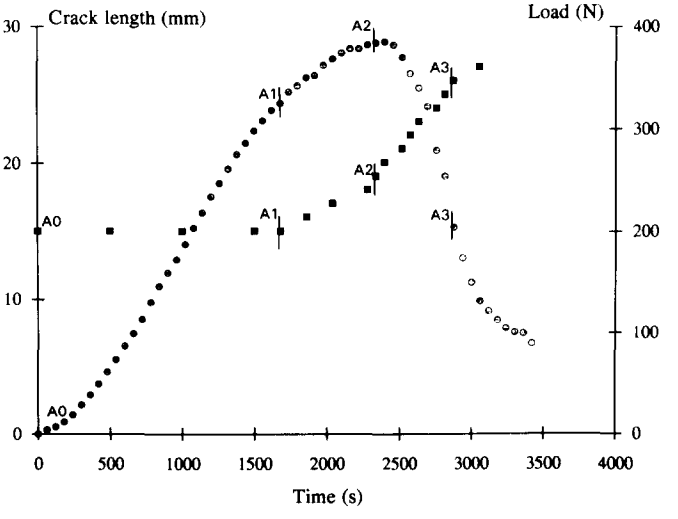

Fig. 10. Typical load (●) versus time curve (CLWL technique) and corresponding crack length (■) as a function of time curve.

—from A3 to the end: the microcracked front reaches the limit of the specimen. The macrocrack only continues to go through the material, so that, from this point A3, information has no more meaning.

The actual crack versus time dependence is presented in Fig. 11: the first slope can be correlated with nucleation and growth of the microcracked area, which appears close to the notch and the second one is attributed to the macrocrack propagation.

From Figs 10 and 11 and taking into account the following relations:[5]

$$K_1 = \frac{P}{B\sqrt{w}} \times f\left(\frac{a}{w}\right)$$

and

$$f\left(\frac{a}{w}\right) = \frac{(2 + a/w)(0{\cdot}886 + 4{\cdot}64(a/w) - 13{\cdot}32(a/w)^2 + 14{\cdot}72(a/w)^3 - 5{\cdot}6(a/w)^4)}{(1 - a/w)^{3/2}}$$

the R-curve of the material is determined. A typical example is given in Fig. 12.

The mean value of the stress intensity factor, in mode 1, corresponding to the crack initiation, K_{1i}, is $4 \pm 0{\cdot}3\ \mathrm{MPa}\sqrt{\mathrm{m}}$, and the critical stress intensity factor is $11{\cdot}5 \pm 0{\cdot}3\ \mathrm{MPa}\sqrt{\mathrm{m}}$. The comparison of these values with those obtained using the Bluhm's slice model shows that:

—K_{1i} is lower than K_{Ii}, which can be explained by the fact that the CLWL method allows to the microcracked process zone appearing at the top of the main crack to be accessed;

—the values of K_{1c} and K_{Ic} are actually very similar, however, it is important to note that the rising R-curve effect is clearly emphasized, thanks to the CLWL test.

The values of K_c are relatively high,[6] owing to a

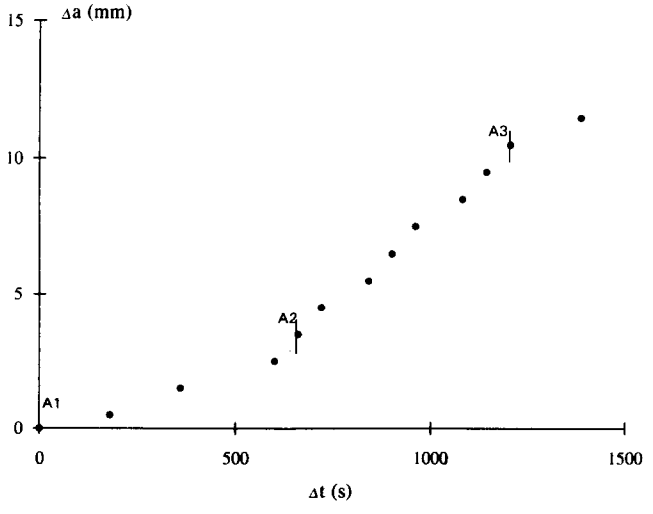

Fig. 11. Crack growth as a function of time, considering the phenomenon initiation as the origin of time (CLWL technique).

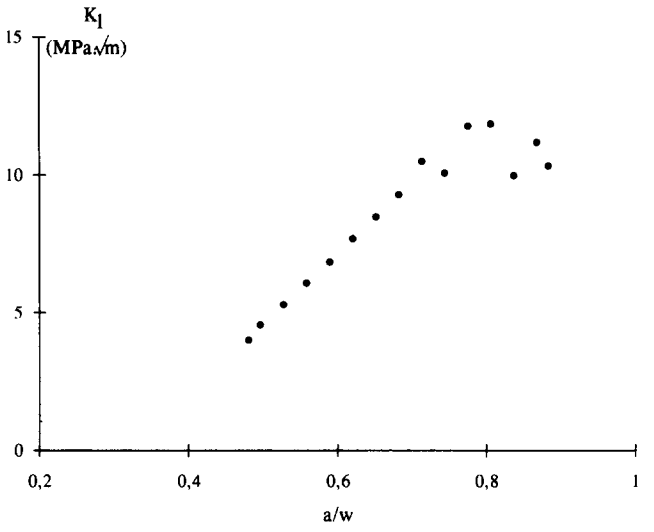

Fig. 12. Typical CLWL R-curve showing crack resistance increase for the Ce-zirconia ceramic.

combination of two reinforcing effects: indeed, in addition to the reinforcement obtained by tetragonal to monoclinic phase transformation, the largely developed microcracking that is observed, also plays a significant role, as shown by fracture faces (Fig. 13), which reveal almost only intercrystalline cracking. Those two mechanisms are well known as main contribution to the enhancement of R-curve behaviour of zirconia-reinforced ceramics.[7,8]

Such an improved crack resistance occurs, however, at the expense of elastic constants (E and G) and of the modulus of rupture.[9,10] This behaviour is attributed mainly to intergranular cracks due to a too high tetragonal to monoclinic transformation ratio during cooling after sintering. Specifically, the strength resistance decrease is also emphasized by the autocatalytic stress-induced martensitic tetragonal to monoclinic transformation[11] (involved in the toughening reinforcement), which occurs during loading. This effect is favourable to microcrack formation and responsible for colour contrasts in the material.

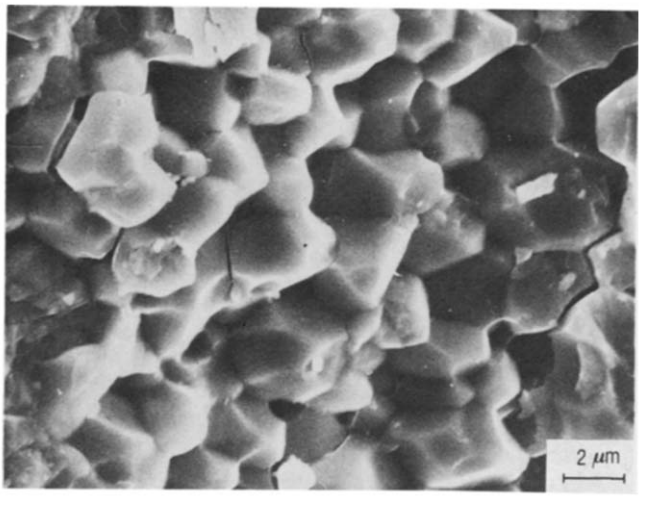

Fig. 13. Fracture face of Ce-zirconia CLWL specimen.

5 Conclusions

The crack line wedge loading (CLWL) method was adapted to the characterization of ceramic materials. It allows the *R*-curve, with stable crack growth, under pure mode 1, to be determined. This technique was applied to the study of a ceria-partially stabilized zirconia.

It was shown, on one hand, that reinforcement mechanisms can be highlighted using the CLWL technique, and on the other hand, that true intensity factor values ban be measured both in the starting crack regime and close to the critical crack propagation limit.

Moreover, the CLWL method allowed the actual values of the stress intensity factor to be detained, because it was possible to take into account both the main crack and the microcracks constituting the process zone.

Although the Ce-zirconia ceramic showed good crack resistance, modulus of rupture and elastic constants were relatively weak as a consequence of microcracking occurring, either during the cooling step after sintering, or during loading.

Acknowledgements

The authors wish to thank C. Cazzaro, J. C. Moulin and J. Dutrieux for their technical assistance.

References

1. Calomino, A. M. & Brewer, D. N., Controlled crack growth specimen for brittle systems. *J. Am. Ceram. Soc.*, **75**(1) (1992) 206–8.
2. Smith, D. K. & Newkirk, H. W., The crystal structure of baddeleyite (monoclinic ZrO_2) and its relation to polymorphism of ZrO_2. *Acta Cryst.*, **18**(6) (1965) 983–91.
3. Weibel, E. R., *Stereological Methods. Vol. 1: Practical Methods for Biological Morphometry*. Academic Press, London, 1979, p. 51.
4. Munz, D., Bubsey, R. T. & Shannon Jr, J. L., Fracture toughness determination of Al_2O_3 using four-point-bend specimens with straight-through and chevron notches. *J. Am. Ceram. Soc.* **63**(5–6) (1980) 300–5.
5. ASTM Designation E561-81. Standard practice for *R*-curve determination.
6. Tsukuma, K., Mechanical properties and thermal stability of CeO_2 containing tetragonal polycrystals. *Am. Ceram. Soc. Bull.*, **65**(10) (1986) 1386–9.
7. McMeeking, R. M. & Evans, A. G., Mechanisms of transformation-toughening in brittle materials. *J. Am. Ceram. Soc.*, **65**(5) (1982) 242–6.
8. Evans, A. G. & Faber, K. T., Crack-growth resistance of microcracking brittle materials. *J. Am. Ceram. Soc.*, **67**(4) (1984) 255–60.
9. Heussner, K. H. & Claussen, N., Strengthening of ceria-doped tetragonal zirconia polycrystals by reduction-induced phase transformation. *J. Am. Ceram. Soc.*, **72**(6) (1989) 1044–6.
10. Tsukuma, K. & Shimada, M., Strength, fracture toughness and Vickers hardness of CeO_2-stabilized tetragonal ZrO_2 polycrystals (Ce-TZP). *J. Mater. Sci.*, **20** (1985) 1178–84.
11. Grathwohl, G. & Liu, T., Crack resistance and fatigue of transforming ceramics: II, CeO_2-stabilized tetragonal ZrO_2. *J. Am. Ceram. Soc.*, **74**(12) (1981) 3028–34.